ANL/MSD-79-7

ANL/MSD-79-7

NONDESTRUCTIVE EVALUATION TECHNIQUES FOR HIGH-TEMPERATURE CERAMIC COMPONENTS

Eighth Quarterly Report
July—September 1979

ARGONNE NATIONAL LABORATORY, ARGONNE, ILLINOIS

Prepared for the Office of Fossil Energy,
U. S. DEPARTMENT OF ENERGY
under Contract W-31-109-Eng-38

DISCLAIMER

Printed in the United States of America
Available from
National Technical Information Service
U. S. Department of Commerce
5285 Port Royal Road
Springfield, VA 22161

NTIS price codes
Printed copy: A03
Microfiche copy: A01

Distribution Category:
Energy Conservation--
Transportation (UC-96)

ANL/MSD-79-7

ARGONNE NATIONAL LABORATORY
9700 South Cass Avenue
Argonne, Illinois 60439

NONDESTRUCTIVE EVALUATION TECHNIQUES FOR HIGH-TEMPERATURE CERAMIC COMPONENTS

Eighth Quarterly Report

July-September 1979

Materials Science Division

October 1979

THIS PAGE

WAS INTENTIONALLY

LEFT BLANK

TABLE OF CONTENTS

LIST OF FIGURES

LIST OF FIGURES (continued)

HIGHLIGHTS

The effect of microstructural variations on ultrasonic flaw detection in silicon carbide has been illustrated for siliconized and α-sintered tubes. The sensitivity of the method for flaw detection is significantly higher in the sintered tube. The variation in velocity of sound as a function of the volume fraction of silicon has been measured experimentally and compared with theoretical calculations. The agreement is reasonably good. Initial results on the use of an acoustic microscope stage for helical scanning of SiC tubes, as well as initial results with the ultrasonic bore-side probe, are presented. A novel dynamic optical technique for surface crack detection is presented and discussed.

NONDESTRUCTIVE EVALUATION TECHNIQUES FOR HIGH-TEMPERATURE CERAMIC COMPONENTS

Eighth Quarterly Report
July-September 1979

D.S. Kupperman, M.J. Caines, D. Yuhas*, C. Sciammarella**, and M. Srinivasan+

I. INTRODUCTION

High-temperature ceramic components are of particular interest because they are lighter than their metallic counterparts, have good corrosion resistance, and can be fabricated from inexpensive and abundant elements. As a result, the use of these ceramics can lead to more efficient energy-conversion systems.

In recent years, significant progress has been made in the use of ceramics for structural applications. Silicon carbide (SiC), for example, is currently being used for heat-exchanger tubing because of its excellent thermal-shock resistance, low coefficient of expansion, high thermal conductivity and strength at high temperature.

The reliable use of ceramics as structural components, however, requires effective failure prediction and thus effective flaw-detection capabilities. The lifetime of SiC components is affected by cracks, porosity, inclusions and free silicon. Many fracture origins are adjacent to the surface[1], indicating that surface cracks are an important cause of failure. The size of critical cracks leading to fracture can be related to microstructural features such as grain size, and can be relatively small (an order of magnitude or more smaller than in comparable metallic parts). Thus, nondestructive evaluation (NDE) techniques that are satisfactory for metals may not be for ceramics. Depending on the component of interest, it may be necessary to develop or advance conventional NDE techniques for ceramic applications. Currently, the techniques most widely employed by industry for ceramic NDE are x-radiography and fluorescent dye penetrant testing. However, efforts are under way at Argonne National Laboratory (ANL) and several other institutions to advance NDE techniques for structural ceramics. The techniques under study outside ANL include high-frequency (> 50 MHz) ultrasonic testing[2], microfocus x-radiography[2], microwave NDE[3], acoustical surface-wave testing[4], photoacoustic microscopy[5], acoustic emission detection[6], and overload proof testing.[7]

*Sonoscan, Inc., Bensenville, IL
**Illinois Institute of Technology, Chicago, IL
+Carborundum Co., Niagara Falls, NY

The purpose of the present ceramic NDE program is to compare the effectiveness of several conventional and unconventional NDE techniques for specific high-temperature ceramic components. The investigation encompasses many NDE techniques, concentrating on those not under extensive evaluation at other institutions. The techniques under study at ANL include dye-enhanced radiography, acoustic microscopy, conventional ultrasonic testing, acoustic-emission detection, acoustic impact testing, holographic interferometry, infrared scanning, internal friction measurements and overload proof testing. No single technique is expected to serve as a universal detection method; several techniques will be required to thoroughly assess ceramic components. After the investigation of many NDE techniques, one or more promising methods will be developed further for the specific ceramic components of interest. The current effort involves SiC heat exchangers; previous efforts have involved silicon nitride gas-turbine rotors.[8]

The current report discusses recent results on inspection of SiC heat-exchanger tubing by means of ultrasonic, acoustic microscopy and holographic interferometry techniques.

II. ULTRASONIC TESTING

A. Effect of Microstructure

The sensitivity of ultrasonic flaw detection is dependent on the microstructure (porosity and grain structure) of the material interrogated. To illustrate this phenomenon, ultrasonic detection sensitivity for essentially identical electric-discharge-machined notches in Carborundum α-sintered and Carborundum KT siliconized SiC tubing (25-mm dia, 3-mm wall) was examined. A lower signal-to-noise ratio for flaw detection was expected for the relatively coarse-grained siliconized material, which produces greater ultrasonic-scattering attenuation. Four ID and OD notches were made in each tube, as indicated in Fig. 1. Figure 2 shows schematically the "1/2 V" beam path used for detecting an ID notch from the OD. All signals from tube J (siliconized) were lower in amplitude than the corresponding signals from tube SRI (α-sintered). Figure 3 compares the signal amplitudes from the no. 5 (500-μm-deep) notches in the two tubes. The notch signal, N, from tube J is about 4 dB lower in amplitude than that from tube SRI. Figure 4 compares the signals from both the no. 5 notches and the shallower (125-μm-deep) no. 6 notches in the two tubes. In the siliconized tube J, the no. 6 notch cannot be separated from the noise, whereas it can in the sintered tube. Clearly, smaller flaws are detectable in the sintered material.

B. Resolution at High Frequency

The sensitivity for flaw detection in structural ceramics is, of course, determined by the wavelength and thus frequency of the ultrasonic beam. A pulser-receiver capable of generating frequencies of up to 75 MHz and a longitudinal-mode 75-MHz transducer have been acquired. The wavelength in SiC at 75 MHz is 160 μm for longitudinal waves and ∿ 100 μm for

shear waves. The advantage of employing these high-frequency, high-resolution waves is illustrated by results obtained on three Knoop dents in a 6-mm-thick hot-pressed silicon nitride bar. The dents, designated B2-1, -2 and -3, measured 500 x 50, 1000 x 25, and 900 x 70 μm, respectively. With 10-MHz, normal-incidence longitudinal waves, none of these dents could be detected. With 10-MHz 45° shear waves, B2-3 could be detected. With 75-MHz normal-incidence longitudinal waves (Fig. 5), all three dents were detectable as ultrasonic signals ahead of the back-wall echo.

C. Silicon Content

The amount of free silicon in siliconized SiC affects its mechanical and thermal properties at high temperature. Ultrasonic techniques may provide a rapid means of measuring the volume fraction of silicon. We have carried out velocity-of-sound measurements on 25 samples of SiC (courtesy of Carborundum), 3 x 6 mm in cross section and about 25 mm long, containing varying amounts of free silicon. If one assumes a composite structure for the material, the average velocity of sound for the sample should be a simple combination of the velocities of sound in the constituent parts. Thus,

$$\frac{1}{v_{ave}} = \frac{1-f}{v_{SiC}} + \frac{f}{v_{Si}}$$

where v_{ave} is the velocity of the composite, v_{SiC} the velocity of sound in fully dense SiC, v_{Si} the velocity of sound in pure silicon, and f the volume fraction of silicon. Rewritten,

$$v_{ave} = \frac{(v_{SiC})\ (v_{Si})}{v_{Si}(1-f)+v_{SiC}f} .$$

For longitudinal waves,

$$v_{SiC} = 12.0 \times 10^5 \text{ cm/s}$$

and

$$v_{Si} = 8.945 \times 10^5 \text{ cm/s} ;$$

from these values, a theoretical dependence of velocity on volume fraction of silicon can be established. The predicted values plus experimental data are presented in Fig. 6. Measurements were made at 10 and 75 MHz to see whether there are any variations associated with wavelength. The scatter in the data is attributed to uncertainties in the volume fraction of silicon, nonuniform distribution of the silicon and slight uncertainties in transient times (∿ 0.5% error). With larger samples, the scatter in the data should be smaller; thus, it is expected that velocity-of-sound data can be used to measure the volume fraction of silicon in SiC to an accuracy

of about ± 15% or better. The discrepancy between calculated and measured velocities is attributed to the simplicity of the model. The anomalous data at f ∿ 0.6 cannot be accounted for at the present time.

D. Use of Bore-side Probe

The bore-side probe for generating longitudinal waves and detecting circumferential laminar-type flaws is shown in Fig. 7. The upper part of the holder contains a 22-MHz probe; the lower part contains a motor for rotating the mirror (center). Figure 8 shows two oscilloscope photographs employing a Sonic Mark III pulser-receiver. The upper trace shows ID and OD echoes for a "normal" part of the tube. The lower trace shows an anomalous region where the ID but not the OD echo is visible. This may be due to defects on the outer surface or porosity in the tube wall, either of which would reduce the reflected signal amplitude. The evaluation of this device is continuing. Some computer hardware has been received and programming has begun for computer interfacing of the probe and pulser-receiver.

III. ACOUSTIC MICROSCOPY

The acoustic microscope stage has been completed and preliminary data acquired for a section of Carborundum KT tubing. Figure 9 shows the stage with the tube in place. A schematic is shown in Fig. 10. The tube is moved axially and/or rotated manually. While the tube moves with respect to the transducer, the acoustic image is viewed on the TV screen. Motion of the tube is about as fast as it would be during examination with an optical microscope. Figure 11 shows an anomalous, highly attenuating region of a tubing section examined with this stage. The system, which now operates at 100 MHz, is being modified to examine tubing at 30 MHz. This will allow a wider field of view and eliminate some of the problems associated with ultrasonic scatter in siliconized tubing.

IV. HOLOGRAPHIC INTERFEROMETRY

A novel holographic method has been developed for the optical detection of cracks on the order of 100 μm in size. Figure 12 schematically illustrates the working principle. Laser light impinges on the surface of the cracked sample in the normal direction and is reflected specularly. If the surface is at rest, most of the light is reflected normal to the surface. However, if the sample vibrates, different surfaces are exposed at the crack opening which reflect light in other directions.

The light from the surface is received by a holographic plate, which collects a time-averaged intensity. We can think of the resultant hologram as representing the surface at the position where the speed of vibration is zero. Consequently, during the reconstruction, the intensity distribution of the light will be related to the amplitude of vibration. If we put the reconstructed hologram in an optical filtering system (Fig. 13) in the Fourier plane of the lens, we obtain the Fourier transform of the intensity distri-

bution for all points on the surface. Under normal illumination and observation, most of the intensity will be concentrated in the zero-order region (Fig. 14). Since the lens collects the intensity from all points on the surface, the intensity that we receive is the sum of the intensities of the transforms of all the points. We can think of the transforms corresponding to all stationary points as being of the same shape. If a point on the surface vibrates, some of the light intensity will be shifted to higher diffraction orders and the transform will be changed. If we insert a window which controls the frequencies that can pass through, then by changing the position of the window, we can control the intensity received by a point observed in the image plane of the filtering system. The points that have experienced displacements due to vibration will appear darker than neighboring points. If the window is moved, the effect becomes dynamic and the eye can easily capture the regions of maximum amplitude of vibration.

This technique has been tested in a ceramic bar with a crack 100 μm long and ∿ 50 μm in depth. The setup is shown schematically in Fig. 15. The ceramic bar is excited in a bending mode at the resonant frequency of 13.6 kHz by means of a piezoelectric transducer. A magnifying optical system is utilized at 30X to produce a lens hologram. Two knife edges, displaced by means of screws, serve as the window-limiting elements. The change in light intensity produced by the motion of the window outlines the region of the crack root.

V. SUMMARY

The effect of varying microstructure on flaw detectability was demonstrated by comparing ultrasonic signal amplitudes from notches in siliconized and sintered SiC tubes. Signal amplitudes were ∿ 4 dB higher in the sintered material.

Knoop dents with depths as small as 25 μm, not detectable at conventional operating frequency (10 MHz), were clearly resolved by use of a 75-MHz transducer.

The velocity of sound was measured as a function of the volume fraction of silicon in Carborundum KT samples. The results suggest that measurement of the velocity of sound may be adequate for indicating silicon content.

Initial data have been presented on flaw detection in SiC tubing with the bore-side ultrasonic probe and acoustic microscope stage. Preliminary results were encouraging.

A novel dynamic holography technique was demonstrated. A 100 x 50-mm-deep Knoop indent in a SiC bar could clearly be seen by this technique, which is a significant improvement over previous optical methods.

REFERENCES

1. F.F. Lange, Structural Ceramic Materials Under Development, Gas Turbine Conference and Products Show, Houston, TX, March 2-6, 1975, paper 75-GT-107.

2. A.G. Evans, G.S. Kino, P.T. Kuri-Yakub and B.R. Tittman, Failure Prediction in Structural Ceramics, Mater. Eval. 35 (4), 85 (April 1977).

3. A.J. Bahr, Microwave Techniques for Nondestructive Evaluation of Ceramics, Final Report AMMRC-CTR-77-29, SRI International, Menlo Park CA (Nov. 1977).

4. B.T. Kuri-Yakub, Acoustic Surface Wave Scattering: The Detection of Surface Cracks in Ceramics, Report SC5064-2TR, Rockwell International Science Center, Thousand Oaks, CA (Dec. 1977).

5. Y.H. Wong and R.L. Thomas, Laser Photoacoustic Techniques for NDE, presented at ARPA/AFML Review of Progress in Quantitative NDE, Scripps Institution of Oceanography, La Jolla, CA (July 12-21, 1978).

6. A.G. Evans and M. Linzer, Failure Prediction in Structural Ceramics Using Acoustic Emission, J. Am. Ceram. Soc. 56 (11), 575 (1973).

7. J.E. Ritter, Proof Testing of Ceramics, 81st Annual Meeting of the American Ceramic Society, Cincinnati, Ohio, April 29-May 2, 1979, paper 14-SC-79.

8. D.S. Kupperman, C. Sciammarella, N.P. Lapinski, A. Sather, D. Yuhas, L. Kessler, and N.F. Fiore, Preliminary Evaluation of Several NDE Techniques for Silicon Nitride Gas-Turbine Rotors, Argonne National Laboratory Report ANL-77-89 (Jan. 1978).

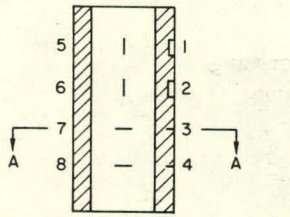

TUBE DIAM. 25 mm
WALL THICKNESS 3 mm

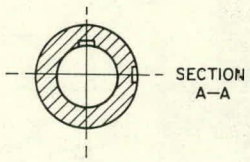

NOTCH*	TYPE	LENGTH (μm)	DEPTH (μm)
1	OD	1250	500
2	OD	250	125
3	OD	1250	500
4	OD	250	125
5	ID	1250	500
6	ID	250	125
7	ID	1250	500
8	ID	250	125

* NOTCH WIDTH 75 μm

Fig. 1. Electric-discharge-machined Notches in SiC Tubes. ANL Neg. No. 306-79-452.

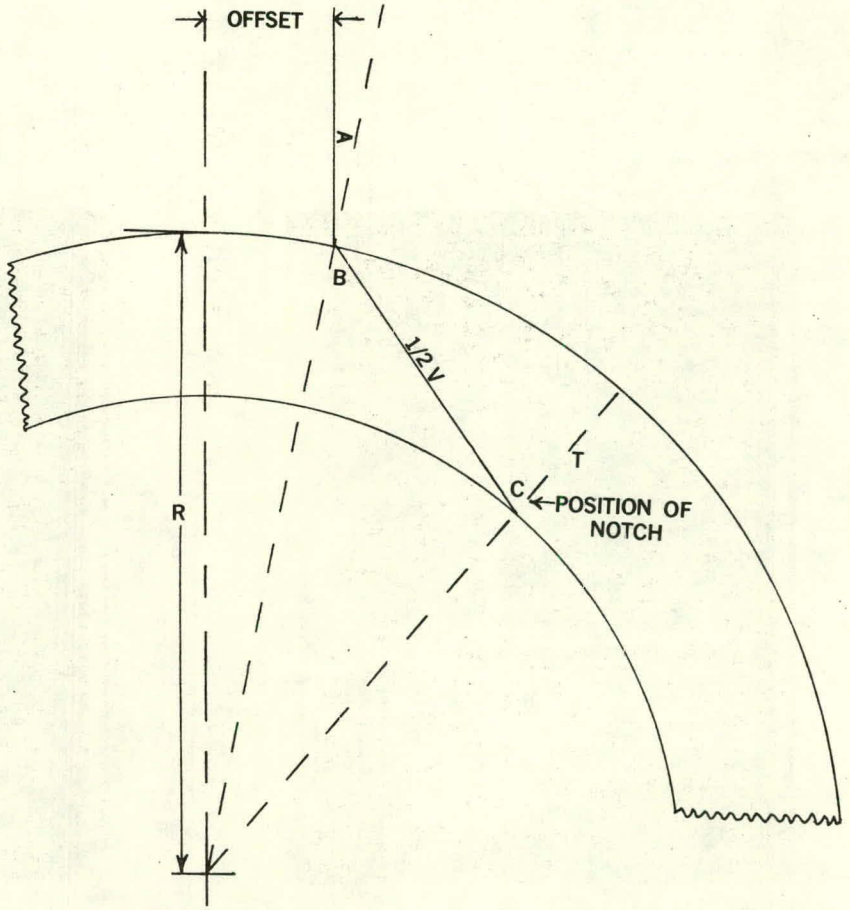

Fig. 2. Cross Section of SiC Tube Showing Offset (1.5 mm), Incident Angle A (7.8°), Refracted Angle B (44.8°), Angle C (70°) Incident to Notch, and Position of EDM Notch for Maximum Reflection (1/2 V Path).

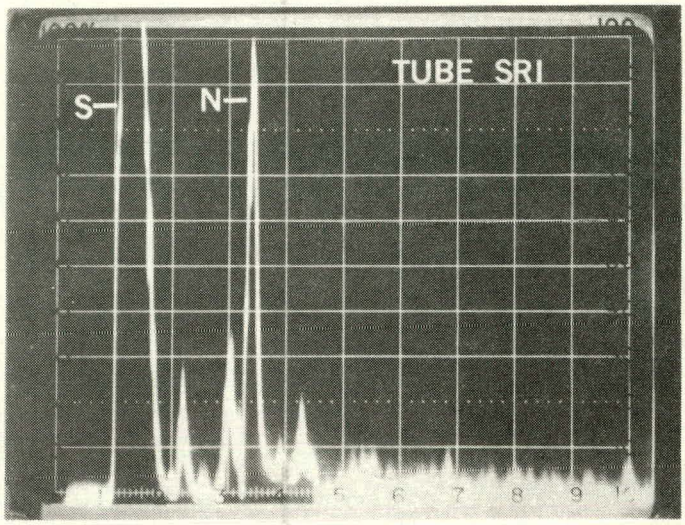

sweep = 0.5 μsec/div.

(a)

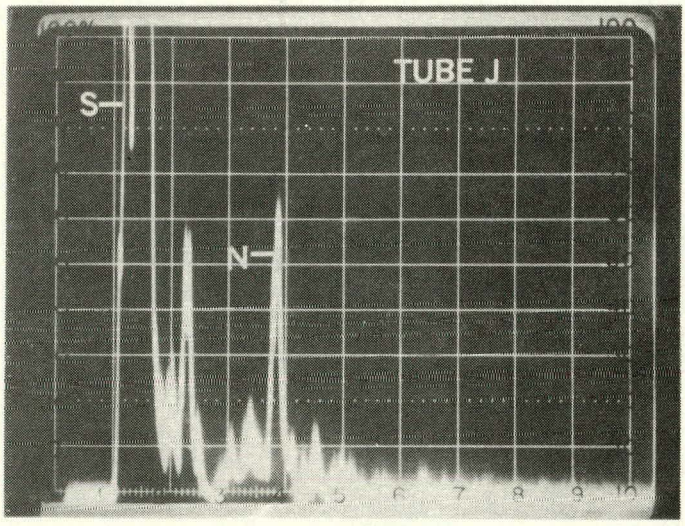

sweep = 0.5 μsec/div.

(b)

Fig. 3. Comparison of Ultrasonic Signal Amplitude for 500-μm-deep Notch in (a) α-Sintered Tube and (b) Siliconized Tube.

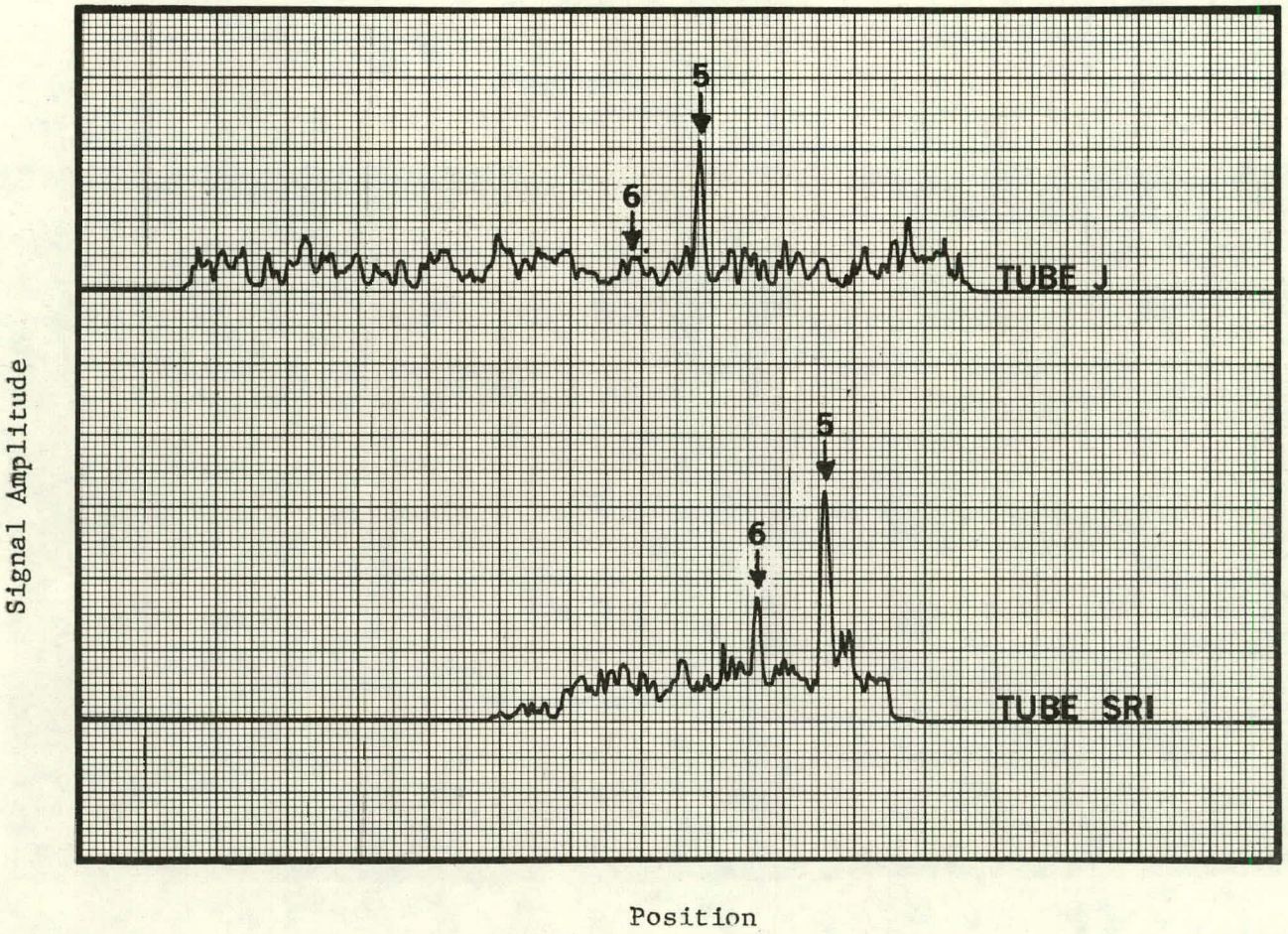

Fig. 4. Axial Scans of Tubes J (Siliconized) and SRI (Sintered), Showing Background Noise and Signals from Notches 5 and 6.

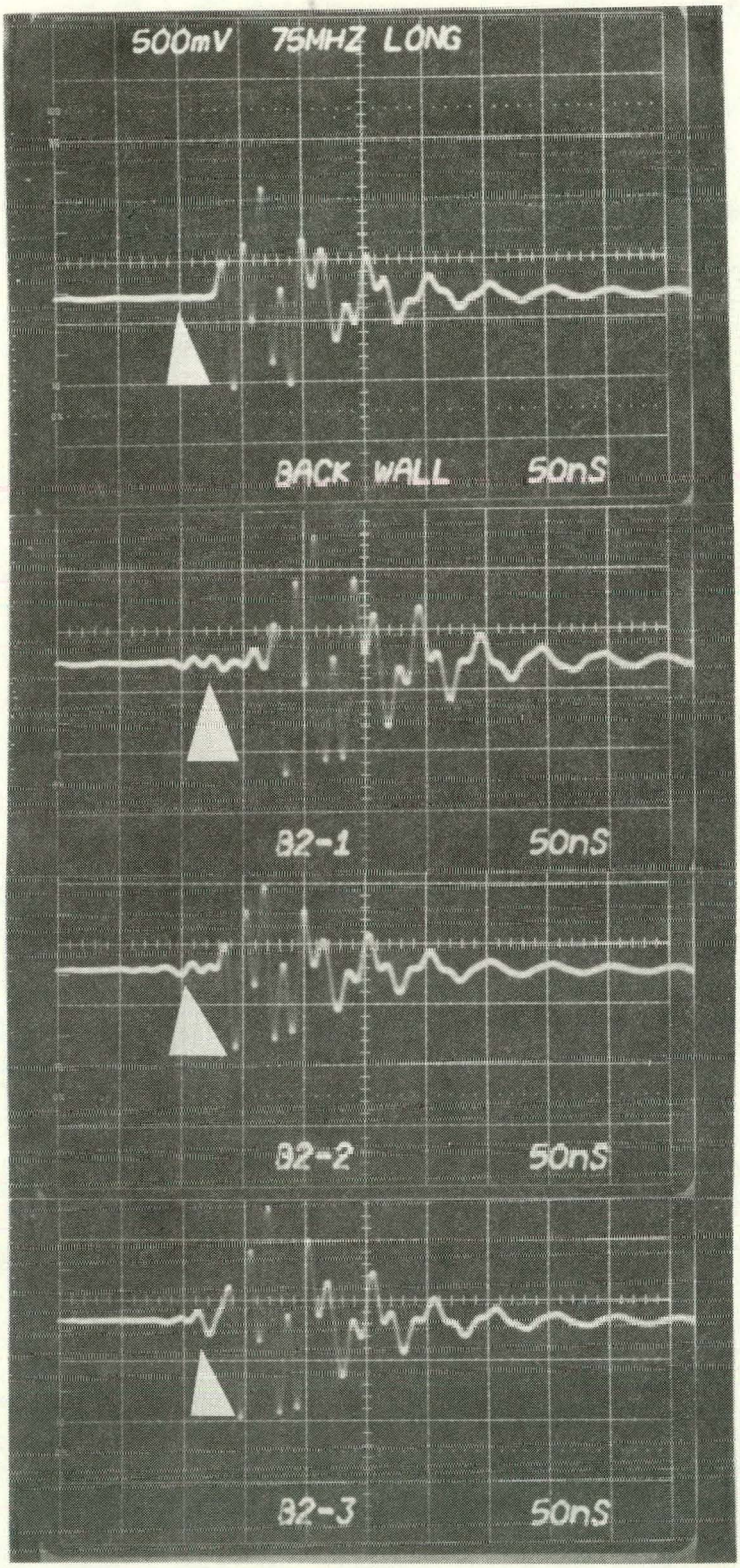

Fig. 5. Detection of Dents in 6-mm-thick Silicon Nitride Bar by Means of 75-MHz Normal-incidence Longitudinal Waves. Dents B2-1, -2 and -3 are 500 x 50, 1000 x 25, and 900 x 70 μm in size, respectively. The dents are detected as radio-frequency signals (arrows) ahead of the back-wall echo. The transducer is 20 mm in diameter.

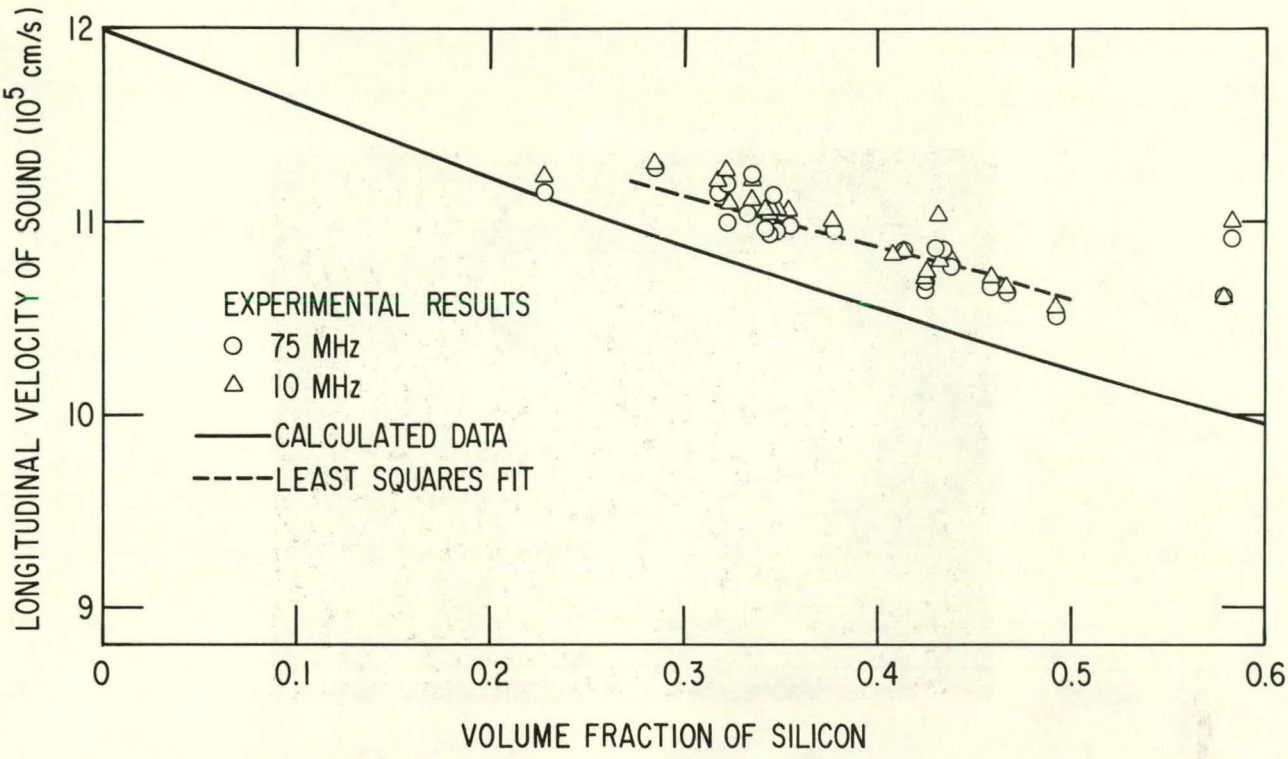

Fig. 6. Velocity of Sound Versus Volume Fraction of Silicon in SiC.

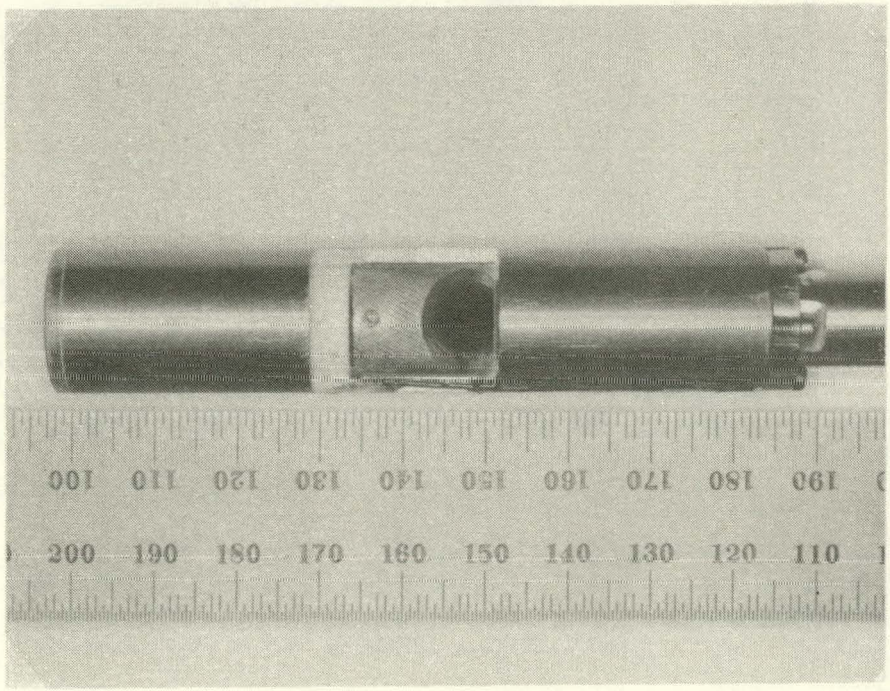

Fig. 7. Bore-side Probe for Flaw Detection in SiC Tubing.

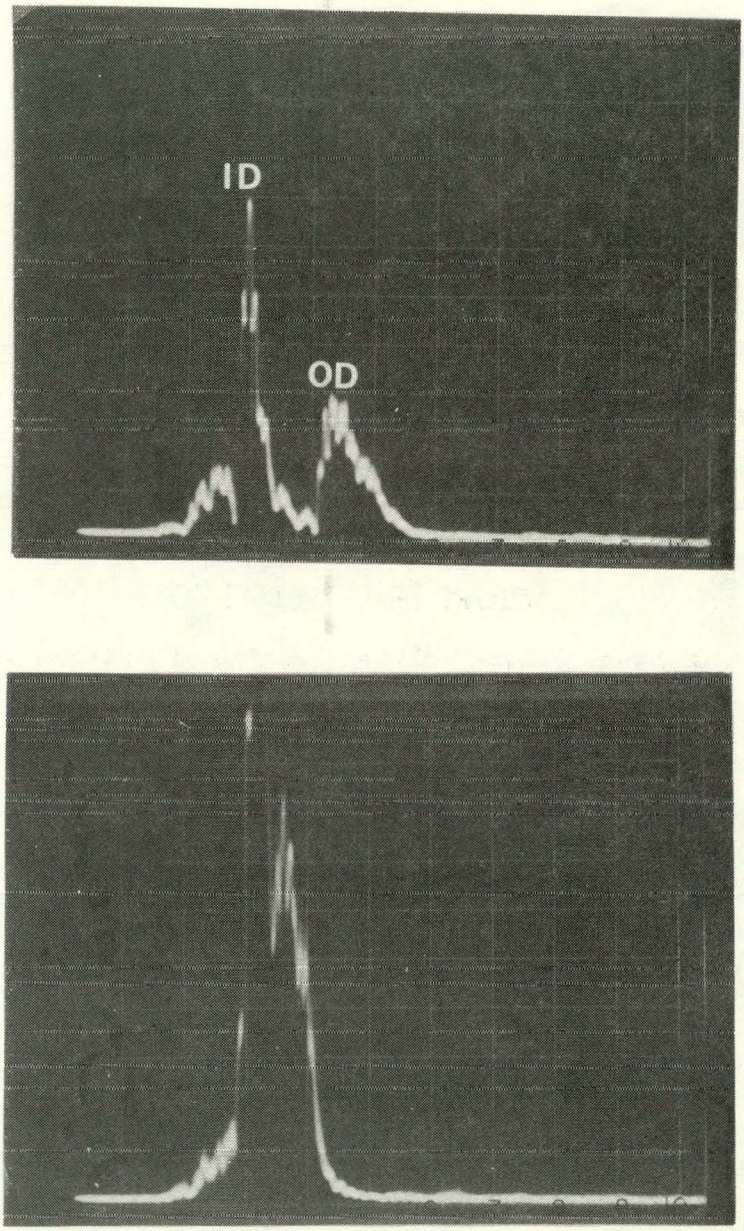

Fig. 8. Oscilloscope Traces Showing Normal (Top) and Anomalous Sections of Carborundum KT SiC Tube.

Fig. 9. Photograph of Acoustic Microscope and Stage for Examination of SiC Tube.

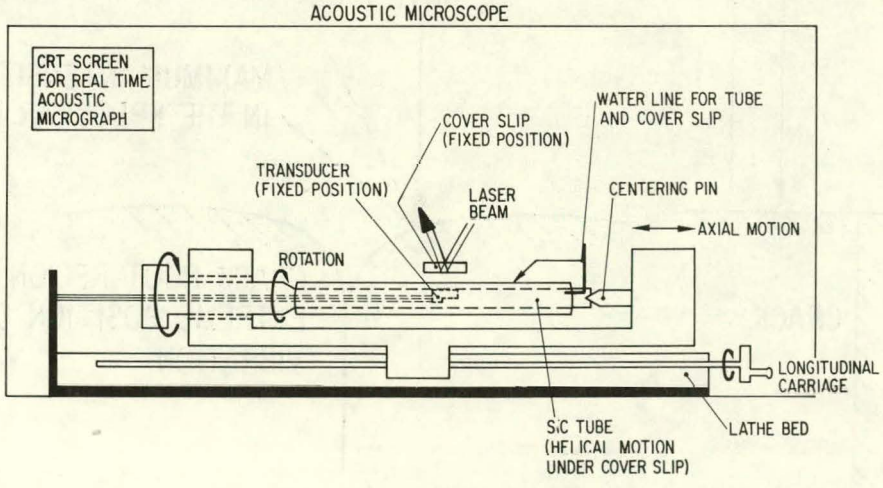

Fig. 10. Schematic of Acoustic Microscope Stage Shown in Fig. 9.

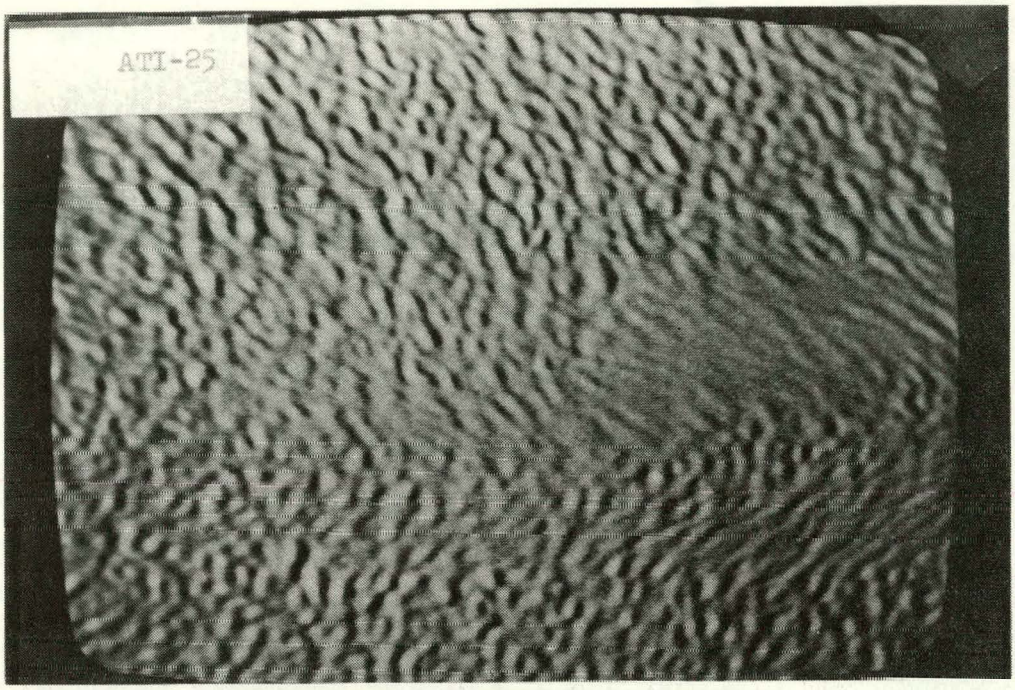

Fig. 11. Acoustic Micrograph of Section of Carborundum KT Tubing, Showing Anomalous Region.

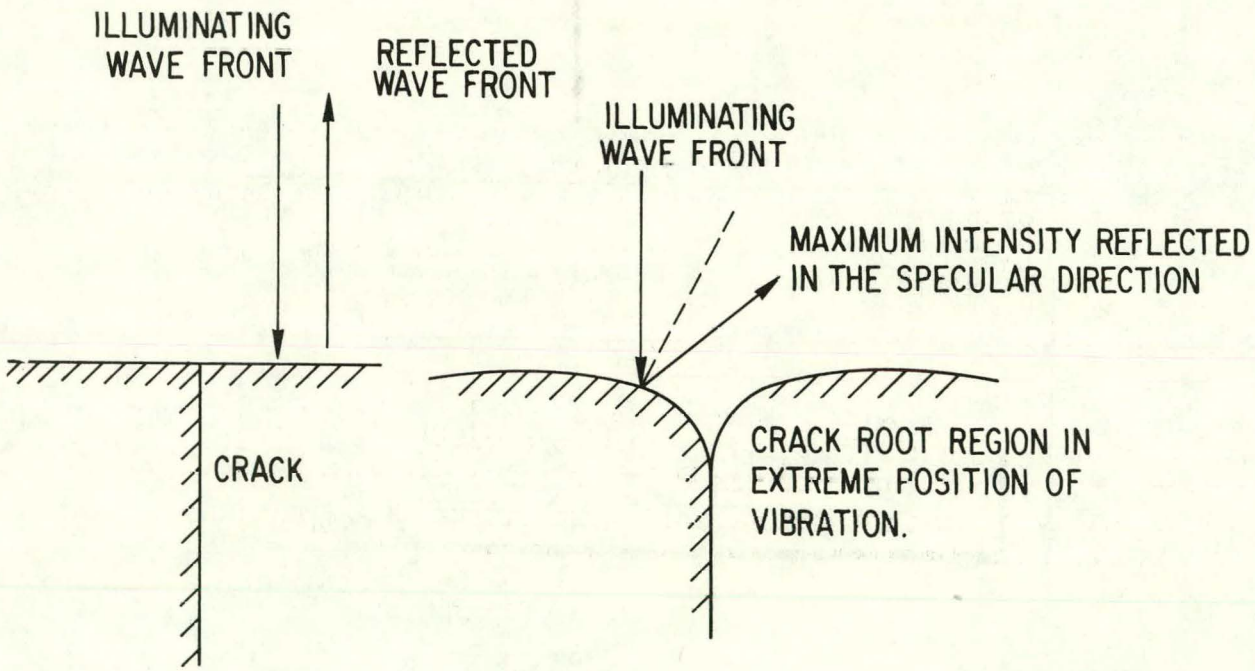

Fig. 12. Schematic Representation of the Dynamic Holographic Technique for Optical Detection of Cracks.

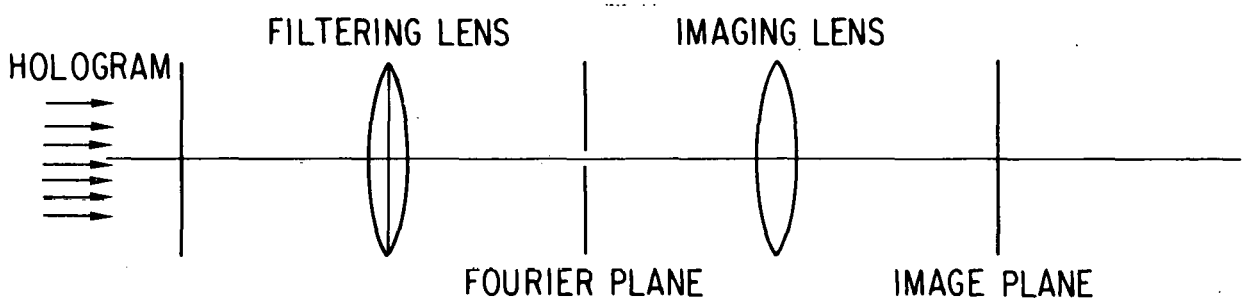

Fig. 13. Schematic Representation of Optical Filtering System.

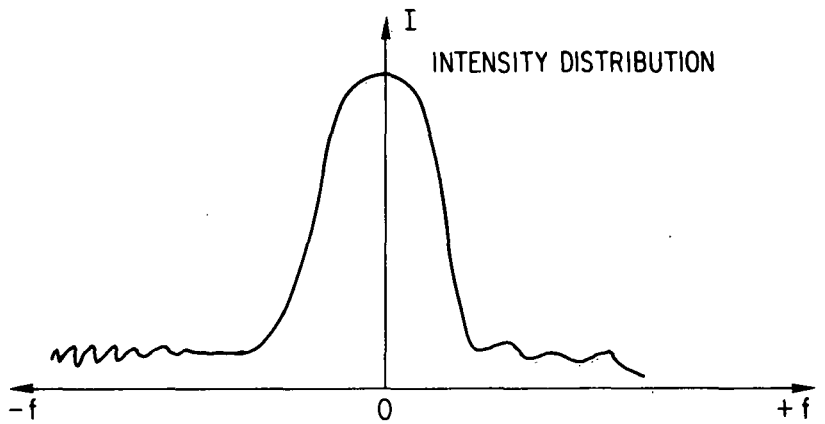

(a)

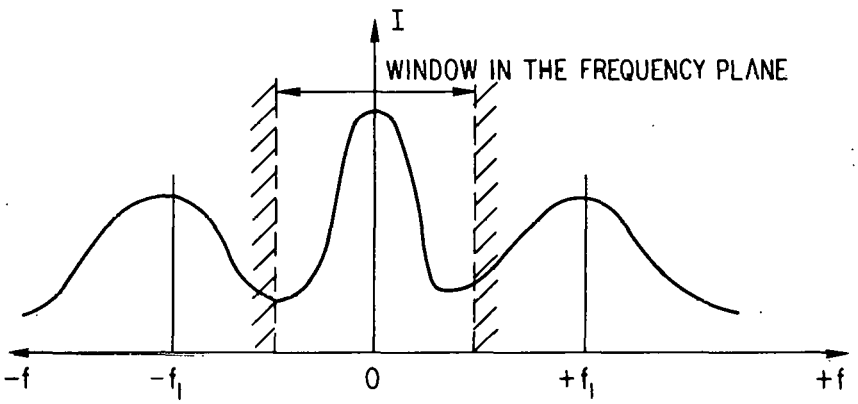

(b)

Fig. 14. Light Intensity Distributions for Points that (a) Remain at Rest and (b) Oscillate.

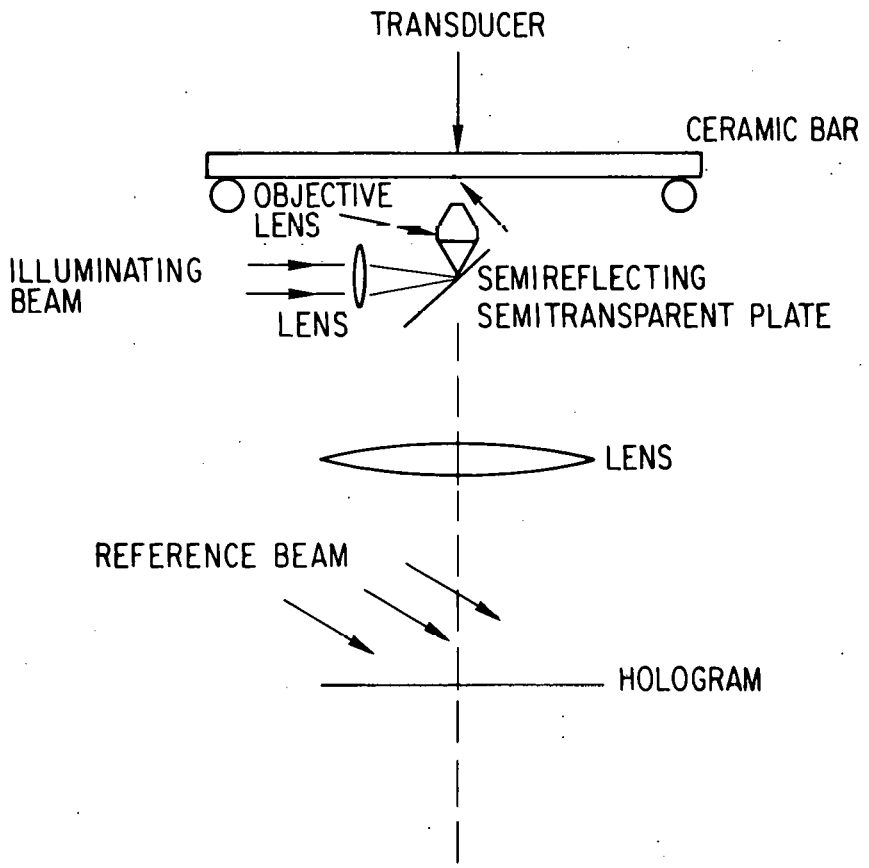

Fig. 15. Schematic Representation of Equipment for Crack Detection with the Dynamic Technique.